

Complementarity of Resonant Scalar, Vector-Like Quark and Superpartner Searches in Elucidating New Phenomena

Anke Biekötter,¹ JoAnne L. Hewett,² Jong Soo Kim,³ Michael Krämer,¹
 Thomas G. Rizzo,² Krzysztof Rolbiecki,⁴ Jamie Tattersall,¹ and Torsten Weber¹

¹*Institut für Theoretische Teilchenphysik und Kosmologie, RWTH Aachen, Germany*

²*SLAC National Accelerator Laboratory, Menlo Park 94025, CA, USA*

³*Instituto de Física Teórica UAM/CSIC, Madrid, Spain*

⁴*Instytut Fizyki Teoretycznej, Uniwersytet Warszawski, Warsaw, Poland*

(Dated: March 5, 2024)

The elucidation of the nature of new phenomena requires a multi-pronged approach to understand the essential physics that underlies it. As an example, we study the simplified model containing a new scalar singlet accompanied by vector-like quarks, as motivated by the recent diphoton excess at the LHC. To be specific, we investigate three models with $SU(2)_L$ -doublet, vector-like quarks with Yukawa couplings to a new scalar singlet and which also couple off-diagonally to corresponding Standard Model fermions of the first or third generation through the usual Higgs boson. We demonstrate that three classes of searches can play important and complementary roles in constraining this model. In particular, we find that missing energy searches designed for superparticle production, supply superior sensitivity for vector-like quarks than the dedicated new quark searches themselves.

CONTENTS

I. Introduction	2
II. Model details	3
The scalar potential	3
The fermion sector	4
Loop-induced Effective couplings	7
III. Results	9
A. Fitting the diphoton signal rate	9
B. LHC Constraints From Searches	12
C. Global Fit	16
IV. Summary	17
Acknowledgments	18
A. Additional decay modes of h_2	18
References	18

I. INTRODUCTION

New physics beyond the Standard Model (SM) might take many forms and, once discovered, will require a complementary multi-pronged attack in order to understand its essential nature. In wider context, as in the case of Dark Matter, this has been recognized for a long time [1]. At the LHC, such an approach will clearly be advantageous no matter what the source of the new physics might be.

In this work, we illustrate the benefits of the complementarity of LHC searches by examining the specific simplified new physics scenario of an additional scalar singlet and a vector-like quark doublet [2, 3], also motivated by the possible signal of a new resonance at 750 GeV [4, 5]. To study this test case, we have combined numerous new physics search channels and analyzed their effectiveness for observing this scenario. In the process, we have found the interesting result that in some cases, the supersymmetry missing transverse energy (MET) based searches perform better in searching for vector-like quarks (VLQs) than the specifically VLQ designed search channels. This provides an explicit example of the interdependency of LHC new physics searches and shows that combining, or recasting, search results would produce improved constraints.

To be specific in defining our scenario, we set the mass of the scalar singlet to be 750 GeV and investigate the possibility that the production and decay of this state is mediated by color-triplet, vector-like quarks [6–9]. More specifically, we will investigate adding a VLQ $SU(2)_L$ doublet whose mass is generated through the vev of the new scalar and which also has Yukawa couplings to the SM fermions via the usual Higgs doublet [10, 11]. In this case, there are three possible charge assignments for the new VLQ fermion states and in order to be concrete, we investigate each of these individually to see if they can reproduce the apparent diphoton production rate. We examine the branching fractions for all relevant possible final states of the scalar resonance in order to ensure that a given model does not produce another signal that would have already been seen.

The presence of the VLQs in this simplified model implies that they can also be produced and searched for directly at the LHC. We consider the possibility that these new states either predominately mix with the first or third generation SM fermions of the same charge. We then apply the existing ATLAS VLQ search at 13 TeV [12] along with a number of ATLAS and CMS supersymmetry searches at both 8 and 13 TeV that are also found to be sensitive to VLQ direct production.

The results obtained in this paper go far beyond those from Ref. [13] where only three 8 TeV searches were included. Using the variety of the most recent searches, including seven at $\sqrt{s} = 13$ TeV (for a total of 105 signal regions), significantly improves the sensitivity to direct VLQ production and decay. In a very recent analysis, Ref. [14], it was also shown that SUSY searches can constrain VLQ models which also contain dark matter particles. With our updated suite of searches we arrive at a similar conclusion in a set of models without dark matter in the final state. In fact, we find that the SUSY searches provide better sensitivity than the dedicated analysis for VLQs in both cases where these new states mix dominantly (but weakly) with either the first or third generation. This is not surprising for first generation mixing since the existing dedicated VLQ search at 13 TeV does not consider this possibility. However the better performance of the supersymmetric search to third generation mixing does motivate the development of improved VLQ searches that make use of missing energy*.

Interestingly, another hint of new physics appears in the ATLAS supersymmetric gluino searches at both 8 and 13 TeV where an on-shell Z -boson is produced together with jets and missing E_T in a cascade decay [16, 17]. Motivated by this possibility, we address a question that has been investigated in the literature as to whether or not the production of VLQ states can simultaneously

* We note that in the finishing stages of this study, ATLAS released a new search with signal regions sensitive to VLQ's that include missing energy [15].

explain both this apparent signal as well as mediate the potential diphoton excess (*e.g.*, [18]). To address this issue in our study we perform a combined fit to both the ATLAS and CMS on-shell Z -boson + MET searches together with a large set of other supersymmetric particle search channels. We find that since the CMS searches for the same final state [19, 20] do not see an equivalent signal, and that once these are combined no significant excess remains in the data.

Our study begins in Sec. II where we present the details of our general model framework and report on the decay rates of the new particles which are relevant for LHC phenomenology. We go further in Sec. III to show the results of a dedicated fit of our model parameters accounting for the benchmark diphoton signal as well as the constraints arising from a large number of other LHC searches. In this section, we also investigate the possibility of explaining the ATLAS on-shell Z + MET excess by the pair production of VLQs. We summarize the results of our analyses in Section IV and in the Appendix A, we provide the formulae for the components of the tree-levels decays of the singlet scalar that are induced by mixing with the SM Higgs.

II. MODEL DETAILS

The specific scenario that we consider is the Standard Model (SM) augmented by a real singlet scalar field together with one additional $SU(2)_L$ doublet of vector-like quarks (VLQs) which are allowed to mix with either the corresponding first or third generation SM quarks through the couplings with the usual Higgs doublet.

The scalar potential

The renormalizable scalar potential for the SM Higgs doublet H plus an additional real singlet scalar S reads [21–24]

$$V(H, S) = -\mu^2 H^\dagger H + \lambda(H^\dagger H)^2 - \frac{\mu_S^2}{2} S^2 + \frac{\lambda_S}{4} S^4 + \frac{\lambda_{SH}}{2} H^\dagger H S^2, \quad (1)$$

with the real quartic couplings λ , λ_S and λ_{SH} and the mass terms μ^2 and μ_S^2 . Both scalars can develop a vacuum expectation value (vev) and H and S can be expanded around their vacuum states as

$$H = \begin{pmatrix} i\phi^+ \\ \frac{1}{\sqrt{2}}(h + v_H + i\phi^0) \end{pmatrix} \quad \text{and} \quad S = (s + v_S), \quad (2)$$

where v_H and v_S are the corresponding vevs with

$$v_H^2 = \frac{2\lambda_S\mu^2 - 4\lambda_{SH}\mu_S^2}{\lambda\lambda_S - 4\lambda_{SH}^2}, \quad (3)$$

$$v_S^2 = \frac{2\lambda\mu_S^2 - 4\lambda_{SH}\mu^2}{\lambda\lambda_S - 4\lambda_{SH}^2}. \quad (4)$$

Note that the scalar potential is Z_2 symmetric, but also that the Yukawa coupling of S to the VLQs, $S\bar{V}V$ given below, will explicitly break this symmetry. The radiatively generated terms S , S^3 and $SH^\dagger H$ all have loop suppressed couplings and can safely be neglected [25]. Using the minimization conditions of the scalar potential, the eigenvalues of the mass matrix of the scalar sector can be expressed in terms of the vevs and the Lagrangian parameters λ , λ_S and λ_{SH} as

$$M_{h_1, h_2}^2 = \lambda v_H^2 + \lambda_S v_S^2 \mp \sqrt{(\lambda_S v_S^2 - \lambda v_H^2)^2 + \lambda_{SH}^2 v_S^2 v_H^2}. \quad (5)$$

The mixing of the interaction eigenstates h and s into the mass eigenstates h_1 and h_2 is described by

$$\begin{pmatrix} h_1 \\ h_2 \end{pmatrix} = \begin{pmatrix} \cos \phi & -\sin \phi \\ \sin \phi & \cos \phi \end{pmatrix} \begin{pmatrix} h \\ s \end{pmatrix}, \quad (6)$$

with the mixing angle given by

$$\tan(2\phi) = \frac{\lambda_{SH} v_S v_H}{\lambda_S v_S^2 - \lambda v_H^2}. \quad (7)$$

We define ϕ such that for $\phi = 0$, the lighter eigenstate corresponds to the SM-like Higgs boson. The couplings of $h_1(h_2)$ to the SM particles are suppressed by $\cos \phi(\sin \phi)$ for non vanishing ϕ and thus the SM Higgs boson has reduced couplings. However, the Higgs coupling measurements are consistent with the SM expectation and hence a strict limit on the mixing angle can be derived from the LHC Higgs data. There are also direct limits from searches of heavy Higgs bosons at the LHC, in particular decays into the SM gauge bosons. In addition, the presence of a heavy scalar can influence electroweak precision data. In a closely related model, Ref. [3] derives an upper limit on this mixing of $|\phi| \lesssim 0.35$.[†]

In the following, we choose to work with the physical masses and mixing angles instead of the parameters of the scalar potential in Eq. (1). To be concrete, we choose the input parameters as

$$M_{h_1} = 125 \text{ GeV}, M_{h_2} = 750 \text{ GeV}, v_H = 246 \text{ GeV}, v_S, \phi. \quad (8)$$

The other parameters are then fixed by the mass formula and the minimization conditions. To conclude this subsection we briefly discuss the perturbativity constraints on our quartic couplings. We perform our numerical analysis in terms of the phenomenological parameters such as the physical masses and the mixing angles. However, for specific values of the masses and the mixing angle, the parameters of the scalar sector can become non-perturbative. We have explicitly checked that all three quartic couplings given above are well below $\sqrt{4\pi}$ in our numerical analyses.

The fermion sector

Here we consider only VLQs in $SU(2)_L$ doublet representations, further demanding that the VLQs can have Yukawa couplings to the corresponding SM fermions via the SM Higgs which then results in only three possible $SU(2)_L$ doublet representations [26]; these are summarized in Table I. After electroweak symmetry breaking (EWSB), the electric charges of the new VLQs that we consider are given by $Q_X = \frac{5}{3}$, $Q_T = \frac{2}{3}$, $Q_B = -\frac{1}{3}$ and $Q_Y = -\frac{4}{3}$. The weak and mass eigenstates associated with the electric charge $\frac{5}{3}$ and $-\frac{4}{3}$ states are equivalent since we assume that only one VLQ $SU(2)_L$ doublet is present in our scenario and there are no corresponding SM states with which these charges can mix. However, the new states T and B will mix with the up-type and down-type SM quarks, respectively. Here we will assume that this mixing involves *either* the first or the third generation quarks only.

[†] Later we will see that we have to choose a very small value for this mixing angle which is well below these experimental limits in order to obtain a sufficiently large branching ratio into diphotons for the heavy scalar.

VLQ model	Representation
(X, T)	$(3, 2, \frac{7}{6})$
(T, B)	$(3, 2, \frac{1}{6})$
(B, Y)	$(3, 2, -\frac{5}{6})$

Table I. Possible vector-like quark doublets assuming possible Yukawa couplings to SM quarks via the usual Higgs doublet and their hypercharges.

As a specific example we consider in detail the case of the (X, T) doublet here. The other VLQ doublet cases follow in a straightforward manner. The most general gauge-invariant Yukawa and mass Lagrangian for the vector-like fermions and the SM up-type quarks of either the first or third generations is given by

$$\mathcal{L}_{\text{Yuk+mass}} = \lambda_u \bar{Q}_L H u'_R + \lambda' (\bar{X}, \bar{T})_L H u'_R + \lambda'' (\bar{X}, \bar{T})_L \begin{pmatrix} X \\ T \end{pmatrix}_R S + m_D (\bar{X}, \bar{T})_L \begin{pmatrix} X \\ T \end{pmatrix}_R + \text{h.c.}, \quad (9)$$

where the prime denotes the weak interaction eigenstates. The Lagrangian for the corresponding (B, Y) model can be obtained upon the following substitutions: $X \rightarrow Y$, $T \rightarrow B$, $u \rightarrow d$ and $H \rightarrow \tilde{H}$, where $\tilde{H} = i\sigma_2 H^*$. For the (T, B) doublet we need to substitute $T \rightarrow B$, $X \rightarrow T$ and $u \rightarrow d$ and also add two additional terms to the Lagrangian

$$\mathcal{L}_{\text{Yuk+mass}} \supset \lambda'_u (\bar{T}, \bar{B})_L \tilde{H} u'_R + m'_D (\bar{u}', \bar{d}')_L \begin{pmatrix} T \\ B \end{pmatrix}_R + \text{h.c.}. \quad (10)$$

For simplicity we consider the mass of the VLQs to be generated by Yukawa couplings to S only, thus we set their both Dirac mass terms to zero $m_D = m'_D = 0$. The mass of the vector-like state X can easily be read off as $m_X = m = \lambda'' v_S$. However, the vector-like T and the SM up quark mix and we can write their mass term as

$$\mathcal{L}_{\text{Yuk+mass}} \supset (\bar{u}, \bar{T})_L \begin{pmatrix} \frac{\lambda_u v_H}{\sqrt{2}} & 0 \\ \frac{\lambda' v_H}{\sqrt{2}} & \lambda'' v_S \end{pmatrix} \begin{pmatrix} u' \\ T' \end{pmatrix}_R = (\bar{u}, \bar{T})_L \mathcal{M} \begin{pmatrix} u' \\ T' \end{pmatrix}_R. \quad (11)$$

Here, in the case of mixing with the first generation u -quark, which we consider first, λ_u is small compared to both λ' and λ'' and can be neglected.

The diagonalization of the mass matrix in this case occurs via a biunitary transformation $\mathcal{M}_{\text{diag}} = U_L^\dagger \mathcal{M} U_R$ and leads to

$$(U_L^\dagger \mathcal{M} U_R)(U_R^\dagger \mathcal{M}^\dagger U_L) = U_L^\dagger \text{diag}(0, \lambda'' v_S + \frac{1}{2} \lambda'^2 v_H^2) U_L, \quad (12)$$

$$(U_R^\dagger \mathcal{M}^\dagger U_L)(U_L^\dagger \mathcal{M} U_R) = U_R^\dagger \mathcal{M}^\dagger \mathcal{M} U_R = U_R^\dagger \begin{pmatrix} \frac{\lambda'^2 v_H^2}{2} & \frac{\lambda' v_H m}{\sqrt{2}} \\ \frac{\lambda' v_H m}{\sqrt{2}} & m^2 \end{pmatrix} U_R. \quad (13)$$

Since the mass matrix in Eq. (12) is already diagonal, we have $U_L = \mathbb{1}$, and only the right-handed particles mix. The corresponding mixing angle, θ_R , is given by

$$\tan(2\theta_R) = -2 \frac{\frac{1}{\sqrt{2}} \lambda' v_H m}{m^2 - \frac{1}{2} \lambda'^2 v_H^2}. \quad (14)$$

For VLQs mixing with instead the third generation of SM quarks, λ_u is no longer much smaller than λ' and λ'' , however the right-handed mixing angle still dominates over the left-handed one, particularly for mixing in the bottom sector [10]

$$\tan(\theta_L) = \frac{m_q}{m_{\text{VLQ}}} \tan(\theta_R). \quad (15)$$

Due to the CKM constraints [27], the mixing with the first generation SM quarks has to be $\mathcal{O}(0.01)$ or less if mixing between the VLQ and left-handed SM fields is allowed. The mixing with the right handed first generation SM quarks is bounded by the couplings of the Z -boson to light quarks which has precisely been measured by LEP [28] and the precision measurements of the atomic parity violation experiments [29]. Using these constraints, limits can be computed on the mixing with right-handed first generation quarks and this must be smaller than $\mathcal{O}(0.1)$ [11].

Limits can also be derived on the third generation mixing angles since the presence of VLQ quarks modifies the oblique parameters S and T [30] as well as the $Zb\bar{b}$ coupling [31]. In the case of the model with a dominant right handed mixing angle for (T, B) , the mixing angle cannot be larger than $\mathcal{O}(0.1)$ [10] and similar constraints are also present for the (X, T) and (B, Y) doublet scenarios.

We note that assuming masses for VLQ states of the order of 800 GeV (as motivated by direct LHC searches), the left-handed mixing angle is already subdominant compared to the right-handed mixing angle even for the top sector. In fact the only effect of the left-handed mixing angle on the phenomenology explored in this study is to modify the branching ratios by $\mathcal{O}(\text{few } \%)$. For VLQ mixing with the SM top quark, the left-handed mixing angle of SM quarks is included in the numerical results. In our analysis we will keep the mixing angle fixed at $\theta_R = 0.01$ for the mixing with either the first or third generation, since its variation below this value will not notably affect the phenomenology of our model.

Upon diagonalization the mass of the heavy new quark T is given by $m_T = \sqrt{m^2 + \frac{1}{2}\lambda'^2 v_H^2} \approx m_X(1 + \frac{1}{2}\theta_R^2)$ so that it would appear that T is heavier than X by ~ 50 MeV if $m_X \sim 1$ TeV. At the 1-loop level, however, the masses of the vector-like quarks receive electroweak radiative corrections, leading instead to $m_X > m_T$, but with $\Delta m = m_X - m_T < 1$ GeV (see Eq. (12) of [32]):

$$m_X - m_T = \frac{\alpha s_W^2 m}{4\pi^2} \frac{5}{3} h \left(\frac{M_Z}{m} \right) \approx \frac{5\alpha s_W^2}{6\pi} M_Z \approx 0.57 \text{ GeV}, \quad \text{with } h(r) \approx 2\pi r, \quad (16)$$

where $s_W = \sin \theta_W$ is the sine of the SM weak mixing angle.

Let us now consider the decays of X and T . Because of its charge, X can only decay via a W boson. The possible decay modes are $X \rightarrow TW^*$ and $X \rightarrow u_R W$. Although the latter mode is suppressed by mixing, it strongly dominates over the decay to a T , because of the small mass difference of the vector-like quarks given above

$$\Gamma(X \rightarrow Tl\nu) = \frac{G_F^2 (\Delta m)^5}{15\pi^3} < 10^{-12} \text{ GeV at } c_R = 1, \quad (17)$$

$$\Gamma(X \rightarrow u_R W) = \frac{G_F m_X^3}{8\sqrt{2}\pi} s_R^2 (1 - r_W)^2 (1 + 2r_W) \approx 1.13 \cdot 10^{-4} \left(\frac{m_X}{700 \text{ GeV}} \right)^3 \left(\frac{s_R}{10^{-3}} \right)^2 \text{ GeV}, \quad (18)$$

where $r_i = m_i^2/m_X^2$ and we denote the sine and cosine of the mixing angle θ_R by $s_R = \sin \theta_R$ and $c_R = \cos \theta_R$, respectively.[‡] The vector-like T can decay to either the SM Higgs or to a Z boson

[‡] A corresponding, but somewhat more complex expression exists when X decays instead to $t_R W$.

plus a SM up-type quark. As long as the mass of the vector-like quarks are well below the mass of the new scalar singlet, T will decay to $T \rightarrow uZ$ and $T \rightarrow uh_1$ with a branching fraction of approximately 50% each, irrespectively of the family to which the VLQs couple. In the case of decays to first generation quarks we find

$$\Gamma(T \rightarrow uZ) = \frac{G_F m_T^3}{16\sqrt{2}\pi} s_R^2 c_R^2 (1 - r_Z)^2 (1 + 2r_Z), \quad (19)$$

$$\Gamma(T \rightarrow uh_1) = \frac{G_F m_T^3}{16\sqrt{2}\pi} s_R^2 c_R^2 \left(c_\phi + \frac{v_H}{v_S} s_\phi \right)^2 (1 - r_{h_1})^2. \quad (20)$$

Because of the assumed absence of a left-handed mixing angle, there is no decay of the T into a W boson. When $m_T > M_{h_2}$, the decay mode $T \rightarrow h_2 u$ opens with a decay width of (again assuming decay to the first generation)

$$\Gamma(T \rightarrow uh_2) = \frac{G_F m_T^3}{16\sqrt{2}\pi} s_R^2 c_R^2 \left(s_\phi - \frac{v_H}{v_S} c_\phi \right)^2 (1 - r_{h_2})^2. \quad (21)$$

We conclude this subsection with a discussion of the (T, B) model which has four mixing angles in the most general case. Again, the left-handed mixing angles are suppressed especially for the case of mixing with the first generation and hence the left-handed mixing angles are not considered as mentioned before. The branching ratios of T and B depend on the mixing angles θ_R^{up} and θ_R^{down} , *e.g.*, the T quark does not couple to the Z and H boson when $\sin \theta_R^{\text{up}} = 0$. Here, we consider a scenario with one mixing angle for the sake of simplicity, and thus we set $\theta_R^{\text{up}} = \theta_R^{\text{down}} = \theta_R$. With this assumption, the couplings of both VLQs in the (T, B) doublet representation to the Z are of the same strength and proportional to $\sin \theta_R \cos \theta_R$. The same conclusion can be drawn for the couplings to the W boson which are also proportional to $\sin \theta_R \cos \theta_R$ [10]. For the Higgs couplings, the relevant interaction terms of the Lagrangian is given by [10]

$$\bar{q} (Y_{qQ}^L P_L + Y_{qQ}^R P_R) QH + h.c.. \quad (22)$$

Here, the couplings Y_{tT}^L and Y_{bB}^L are of the same size, but Y_{qQ}^R differs by a factor $\frac{m_q}{m_Q}$ for the top and bottom quark, respectively.

Loop-induced Effective couplings

The heavy scalar h_2 is mainly produced in gluon-fusion with the vector-like quarks running in the fermion loop assuming a small mixing angle ϕ . At vanishing mixing with the SM Higgs, all the decay modes of h_2 (which then coincides with s) are purely loop-induced assuming the on-shell decays to the VLQs are closed. The interaction of the new scalar with the vector bosons is given by the effective Lagrangian

$$\mathcal{L}_{\text{eff}} = -\frac{1}{4} g_{sgg} s G_{\mu\nu} G^{\mu\nu} - \frac{1}{4} g_{s\gamma\gamma} s A_{\mu\nu} A^{\mu\nu} - \frac{1}{4} g_{sZZ} s Z_{\mu\nu} Z^{\mu\nu} - \frac{1}{2} g_{sWW} s W_{\mu\nu} W^{\mu\nu} - \frac{1}{2} g_{sZ\gamma} s A_{\mu\nu} Z^{\mu\nu}, \quad (23)$$

where g_{sxy} denotes the effective coupling to the vector bosons x, y . For gluons and photons these are given by

$$g_{sgg} = \frac{\alpha_s}{4\pi} \sum_{i=X,T} \frac{g_{sii}}{m_i} A_{1/2}(\tau_i), \quad (24)$$

$$g_{s\gamma\gamma} = \frac{\alpha}{4\pi} \left(2N_C \sum_{i=X,T} Q_i^2 \frac{g_{sii}}{m_i} A_{1/2}(\tau_i) \right), \quad (25)$$

where $A_{1/2}$ is the standard loop integral

$$A_{1/2}(\tau) = 2\tau [1 + (1 - \tau) f(\tau)], \quad (26)$$

$$f(x) = \arcsin^2(1/\sqrt{x}), \quad (27)$$

with $\tau_i = 4m_i^2/m_s^2$. The couplings of the scalar s to the VLQs are given by

$$g_{sTT} = \frac{m_T}{v_H} \left(s_R^2 s_\phi + \frac{v_H}{v_S} c_R^2 c_\phi \right), \quad (28)$$

$$g_{sXX} = \frac{c_\phi c_R m_T}{v_S}. \quad (29)$$

Neglecting the squares of the mass of the W and the Z bosons relative to that of the s , the effective couplings of the scalar s to $Z\gamma$, ZZ and WW are given by [6, 33]

$$g_{sZZ} = \frac{\alpha}{4\pi} \left[\frac{2N_C}{s_W^2 c_W^2} \sum_{i=X,T} (I_i^3 - s_W^2 Q_i)^2 \frac{g_{sii}}{m_i} A_{1/2}(\tau_i) \right], \quad (30)$$

$$g_{sZ\gamma} = \frac{\alpha}{4\pi} \left[\frac{2N_C}{s_W c_W} \sum_{i=X,T} Q_i (I_i^3 - s_W^2 Q_i) \frac{g_{sii}}{m_i} A_{1/2}(\tau_i) \right], \quad (31)$$

$$g_{sWW} = \frac{\alpha}{4\pi} \left[\frac{N_C}{2s_W^2} \sum_{i=X,T} \frac{g_{sii}}{m_i} A_{1/2}(\tau_i) \right]. \quad (32)$$

In Table II we give some values for the resulting branching ratios of s for the different VLQ doublets. We take into account a K-factor of 1.638 [34] for the production of s via gluon fusion at 13 TeV and a K-factor of $1 + 67\alpha_s(M_{h_2})/4\pi$ for the decay into two gluons.[§]

Additional decay modes can be induced by the mixing with the SM Higgs boson and these lead to a tree level contribution to WW and ZZ final states. We provide the explicit formulae for the component of the tree-level decays induced by mixing with the SM Higgs in the Appendix A. We also note that while our formulae neglect the interference between the loop-induced couplings and those arising from mixing with the SM Higgs, all of our numerical results include such effects. An additional contribution could also come from the mixing with the SM-quarks, but in our case this effect is negligible due to the small values of the relevant mixing angles $\theta_{L,R}$.

For the numerical analysis, we implemented the three models using `FeynRules2.3.18` [36, 37]. We validated our implementation by comparing our results to the kinematic distributions as depicted in the ATLAS search for VLQs [12].

VLQ model	Representation	$\gamma Z/\gamma\gamma$	$ZZ/\gamma\gamma$	$WW/\gamma\gamma$	$gg/\gamma\gamma$	$\Gamma_{s \rightarrow \gamma\gamma}$ [MeV]	Γ_{Tot} [MeV]	$R_{\gamma\gamma}$ [fb]
(X, T)	$(3, 2, \frac{7}{6})$	0.07	0.59	0.90	17.0	1.03	20.0	6.2
(T, B)	$(3, 2, \frac{1}{6})$	5.02	9.11	30.2	570.3	0.03	18.8	0.2
(B, Y)	$(3, 2, -\frac{5}{6})$	0.01	1.21	2.61	49.3	0.35	19.1	2.2

Table II. Branching ratios into various final states of the new scalar s , the total width Γ_{Tot} and the diphoton production rate $R_{\gamma\gamma}$ for the following input parameters: $v_S = 750$ GeV, $\phi = 0$, $m_{\text{VLQ}} = 1$ TeV, $\sin^2 \theta_w = 0.2315$, $\alpha_s(M_s) = 0.09036$.

[§] We employ the results of Ref. [35] with $\mu = m_s$ and $N_f = 6$ which is applicable when $m_i^2/m_s^2 \ll 1$ and $4m_{\text{VLQ}}^2/m_s^2 > 1$.

III. RESULTS

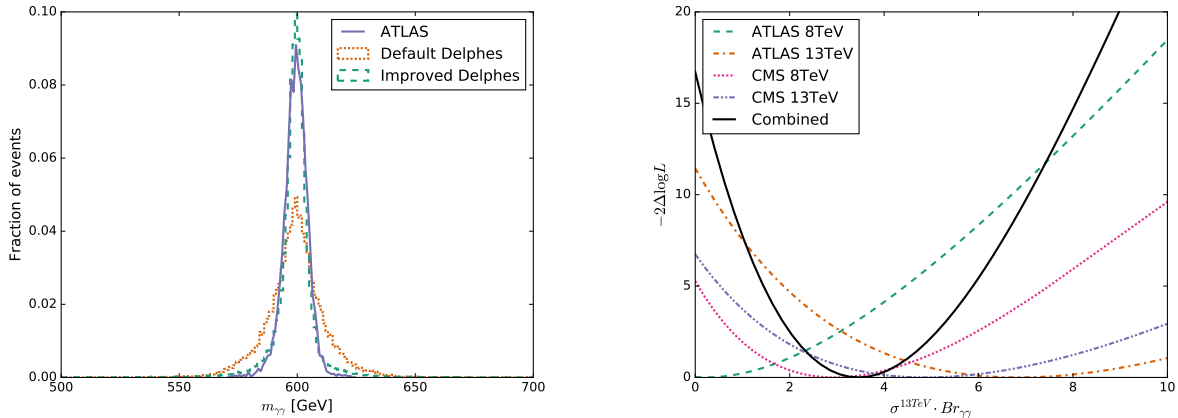


Figure 1. Detector resolution for the ATLAS detector compared with that from Delphes before and after tuning (left). χ^2 of the combined diphoton results as a function of the $\sigma \times \text{BR}(h_2 \rightarrow \gamma\gamma)$. The best fit point lies at $\sigma \times \text{BR} = 3.5 \pm 1.0$ fb. The CMS results are taken from Figure 10 (left) in [5].

We perform a combined fit for the diphoton signal rate and a number of ATLAS and CMS searches which are sensitive to VLQ pair production. For purposes of demonstration, we employ the observed value of the excess diphoton rate at 750 GeV. To compare the results for the pair production of VLQs with a large number of LHC searches we make use of the tool `CheckMATE` [38, 39] including the `Delphes 3` detector simulation [40]. For all analyses, the anti- k_T jet algorithm is used [41–43] and we also include additional, externally implemented analyses [44]. For each of the various signal regions we compute a likelihood by assuming that the various systematic uncertainties are distributed according to a Gaussian probability density function (PDF) and combine this with the Poisson distributed statistical uncertainty. Each analysis likelihood (including the diphoton results) are then combined to give a total χ^2 for the model under test. When combining LHC analyses, we make sure to only include orthogonal signal regions.

To present our results we display the χ^2 relative to that predicted by the SM alone,

$$\chi_{\text{rel}}^2 = -2(\ln L - \ln L_{\text{SM}}) . \quad (33)$$

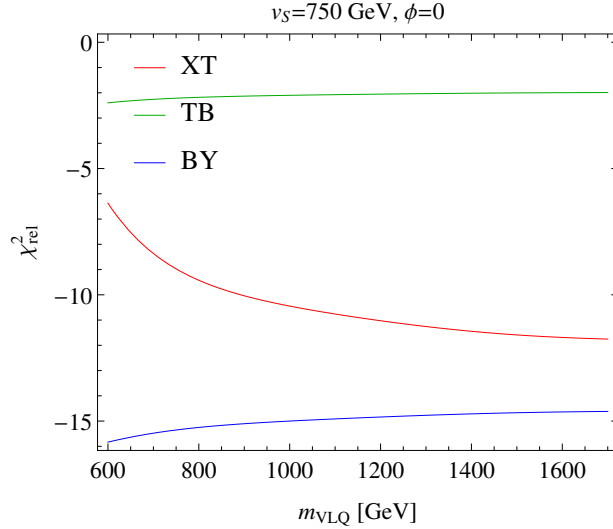
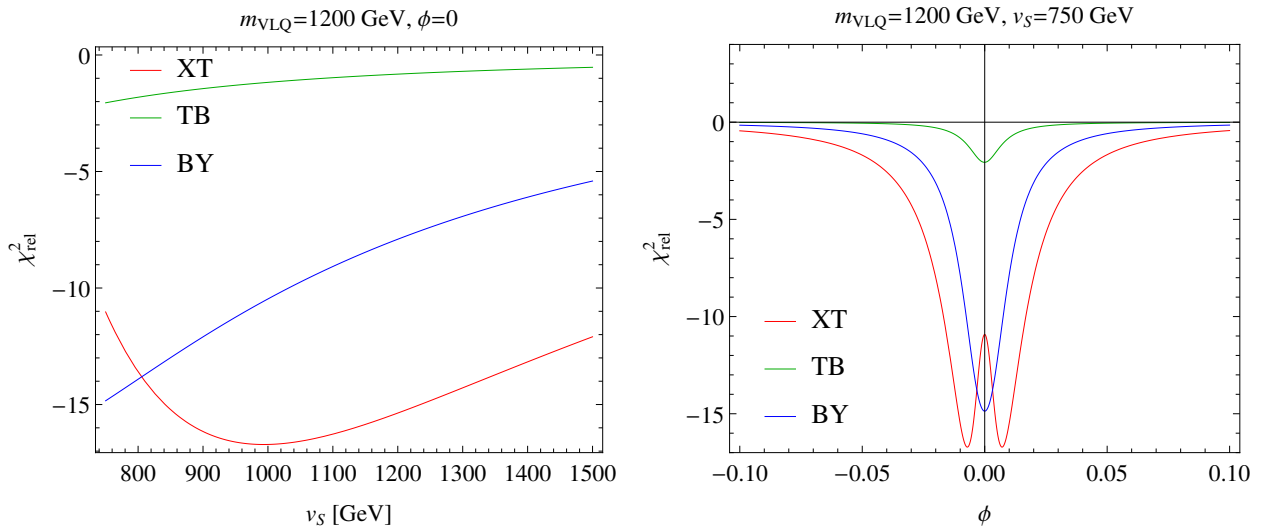
As discussed below, we also investigate all other final states that may be produced by a 750 GeV resonance (as shown in Table IV). However we find that in the models we explore here, none of these are relevant with the currently collected data since the current limits lie far from the anticipated rates.

A. Fitting the diphoton signal rate

We start our analysis of the different VLQ doublets by fitting the likelihood of the excess diphoton signal without taking into account other experimental constraints. We consider the diphoton searches by ATLAS and CMS at 13 TeV and the 8 TeV results scaled to the 13 TeV cross-section [4, 5] in the invariant mass range $m_{\gamma\gamma} \subset [650, 850]$ GeV. We implemented the ATLAS analyses in `CheckMATE` and tuned the Delphes detector card to better reproduce the detector response to photons which is over-smearred in the default Delphes setup, as seen in Fig. 1. The likelihood for CMS is fitted to the values shown in [5]. For a scalar resonance, we find the best fit point for the

Parameter	Range
m_{VLQ} [GeV]	[600, 1800]
v_S [GeV]	[750, 2000]
ϕ	[-0.1, 0.1]

Table III. Range of the parameters varied in the fit.

Figure 2. Comparison of the diphoton fit χ^2 contributions for the different VLQ doublets.Figure 3. Comparison of the fits of vector-like quark doublets for the diphoton likelihood. Variation of the vev of the new scalar v_S (left) and its mixing angle with the SM Higgs ϕ (right).

diphoton rate is $\sigma \times \text{BR} = 3.5 \pm 1.0 \text{ fb}$ (see Fig. 1) and, due to the improved photon response that we have implemented, this value is somewhat below the one commonly shown in the literature [45].

The fit of the diphoton rate is independent of which family of SM quarks primarily couple to the VLQs since we only consider production via gluon fusion. Keeping the mixing angle of the quark sector θ_R fixed (which as stated earlier, has to be small due to CKM constraints), the mass of the VLQs, m_{VLQ} , the vev of the new scalar v_S and the scalar mixing angle ϕ are the parameters

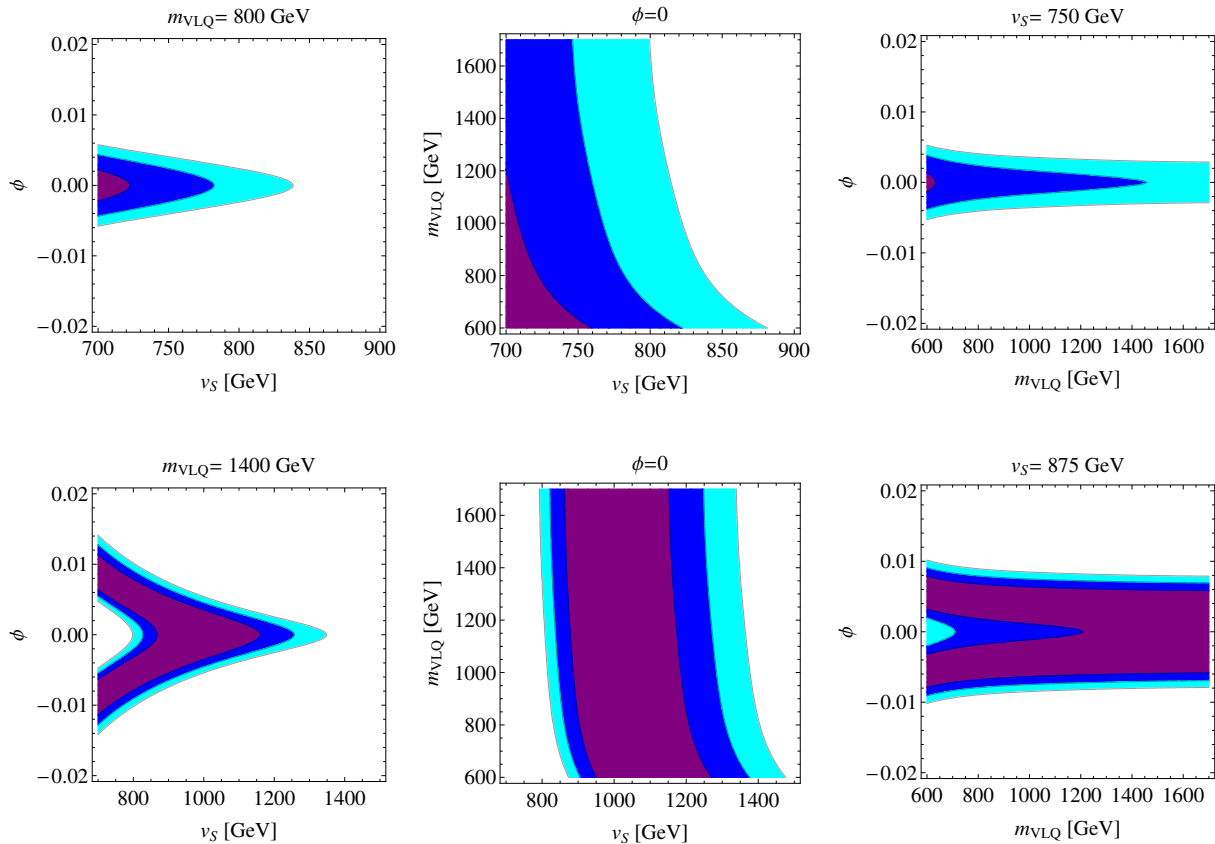


Figure 4. Contours of the likelihood for the (B, Y) (upper) and (X, T) (lower) model for the diphoton rate contribution to the overall χ_{rel}^2 only. The contours are shown for the 1σ (purple), 2σ (dark blue) and 3σ (light blue) regions. Please note the different plot ranges and values for v_S and m_{VLQ} .

that influence the cross section times branching ratio into a pair of photons. For our fit, we vary those parameters in the ranges given in Table III.

We calculate the production cross section of the new scalar h_2 using `MadGraph` [46] including the K-factor of 1.638 as mentioned above and calculate its BRs analytically via Eqs. (24)-(32) and the equations given in App. A. In Fig. 2 the dependence of χ_{rel}^2 on the VLQ mass is given for the different VLQ doublets for $v_S = 750$ GeV and $\phi = 0$. From the behavior of the curves one can see that the cross section times branching ratio for the (T, B) and the (B, Y) model is too small for the given parameter range, whereas in contrast the (X, T) model predicts a too large rate for the diphoton resonance.

As we allow ϕ to vary, the tree level decays $h_2 \rightarrow WW/ZZ/h_1h_1/f\bar{f}$ become possible (and relevant), suppressing the BR of the new scalar to two photons (see Appendix A for the tree-level decay widths of h_2). In addition, in order not to make the Yukawa couplings of the VLQs too large, we only consider the regime $v_S > 750$ GeV. Since a larger v_S corresponds to a smaller Yukawa coupling (for fixed m_{VLQ}), increasing the value of v_S will also lead to a smaller diphoton rate.

Thus increasing either v_S or ϕ in the given range will only worsen the quality of the diphoton fit for both the (T, B) and (B, Y) models, see Fig. 3. However, we note that for very low mass VLQs ($m_{VLQ} \sim 600$ GeV) the diphoton rate as observed by ATLAS and LHC can be reached within 1σ for the (B, Y) model as shown in the upper panel of Fig. 4.

In contrast to the two models already discussed, when $v_S = 750$ GeV and $\phi = 0$, the (X, T) model actually predicts a too large diphoton rate. Consequently the fit can actually now be improved with the variation of v_S and ϕ (see lower panel of Fig. 4). For example, for smaller values of v_S or m_{VLQ} , a non-zero value of ϕ is found to be favored as a way to reduce the diphoton rate and fit the experimental combined result.

B. LHC Constraints From Searches

Additional constraints on the parameters of our models may arise from limits of the decay of the new scalar to final states other than $\gamma\gamma$ as well as from LHC searches that are sensitive to VLQ pair production. Since the mixing angle of the VLQs to SM quarks has to be very small, we find that there are no relevant constraints on our model parameters originating from the single production of VLQs.

We first consider the limits arising from the resonant searches in other relevant final states at 750 GeV. These are presented in Table IV and we find that all of these bounds are presently too weak to place constraints on any of the above models given the parameter ranges that we explore.

Final state	95% CL upper limit on $\sigma \times \text{BR}$ [fb]
WW [47]	180
ZZ [48]	55
jj [49]	2000
$Z\gamma$ [50]	18
hh [51]	198

Table IV. 95% CL upper limits on $\sigma \times \text{BR}$ for different final states. None of these are found to be relevant for the set of models and parameters investigated in this study.

In contrast, the existing limits on the pair production of VLQs can set meaningful constraints on the parameter space. We should first remember that the pair production of vector-like quarks is independent of the properties of the scalar sector v_S and ϕ in the range relevant to fit the diphoton rate ($\phi \in [-0.03, 0.03]$, $v_S \in [750, 1500]$) since their branching ratios depend only very weakly on v_S and ϕ . As long as we keep the mixing angle of the quark sector θ_R fixed, the mass of the VLQs is therefore the only parameter influencing the results for VLQ pair production.

To compare the results for the pair production of VLQs with the set of LHC searches we consider, we again make use of **CheckMATE**. In Table V we display the list of the analyses that are sensitive to VLQ pair production and are taken into account as part of the present study. We include three 8 TeV and seven 13 TeV searches, which when combined corresponds to 105 signal regions in total. For the 95% CLs exclusion we only consider the signal region with the best expected sensitivity and then apply the result using the collected data. When performing the combined fit of analyses, if an analysis has overlapping signal regions we only include the signal region that was expected to be most sensitive from this analysis. Such a procedure applies to all the ATLAS analyses apart from the VLQ search which has orthogonal signal regions. In addition, for analyses that target similar final states, each signal region was examined to make sure that no signal regions overlap. For the final combination we assume no correlations in the systematic uncertainties between signal regions which implies our exclusion is more conservative than if such correlations were included.

We generate our event samples for vector-like quark pair production with **MadGraph** [46] and use **Pythia6** [52] for parton showering. The cross section is computed at NNLO in QCD with **Top++** [53]. In Fig. 5 we compare the likelihood contributions determined by **CheckMATE** for the

8 TeV and 13 TeV analyses combined with the contribution from the diphoton fit. For VLQs coupling to the first generation, we find that the fit results are almost indistinguishable between the different models despite the fact that the branching ratios to different bosons differ substantially for the (T, B) doublet. The VLQs in the (T, B) doublet decay to (W, Z, h) with branching ratios of approximately (50%, 25%, 25%) which roughly agree with the averaged branching ratios of the VLQs in the (X, T) and (B, Y) doublet where one of the VLQs decays exclusively to W bosons and the other decays to Z bosons and h bosons at approximately 50% BR each. However, in the models with third generation mixing, the different branching ratios to top and bottom quarks lead to different signatures at the LHC. Therefore, the results for VLQs coupling to the third generation of SM quarks are only valid for the (X, T) VLQ doublet model explored here.[¶]

Experiment	\sqrt{s} [TeV]	# SRs	Search for
ATLAS	8	15	Squarks and gluinos (jets + E_T^{miss}) [54]
ATLAS	8	1	Squarks and gluinos (same-flavour opposite-sign dilepton pair + jets + E_T^{miss}) [16]
CMS	8	6	Squarks and gluinos (same-flavour opposite-sign dilepton pair + jets + E_T^{miss}) [19]
ATLAS	13	10	Vector-like top quark pairs (1 lepton + jets) [12]
ATLAS	13	8	Gluinos ($> 3b$ -jets + E_T^{miss}) [55]
ATLAS	13	6	Gluinos (1 lepton + jets + E_T^{miss}) [56]
ATLAS	13	7	Squarks and gluinos (jets + E_T^{miss}) [57]
ATLAS	13	4	Squarks and gluinos (2 or 3 leptons + jets + E_T^{miss}) [58]
ATLAS	13	1	Squarks and gluinos (leptonic- Z + jets + E_T^{miss}) [17]
CMS	13	47	Squarks and gluinos (same-flavour opposite-sign dilepton pair + jets + E_T^{miss}) [20]

Table V. List of the analyses with brief descriptions included in the fit of VLQ pair production.

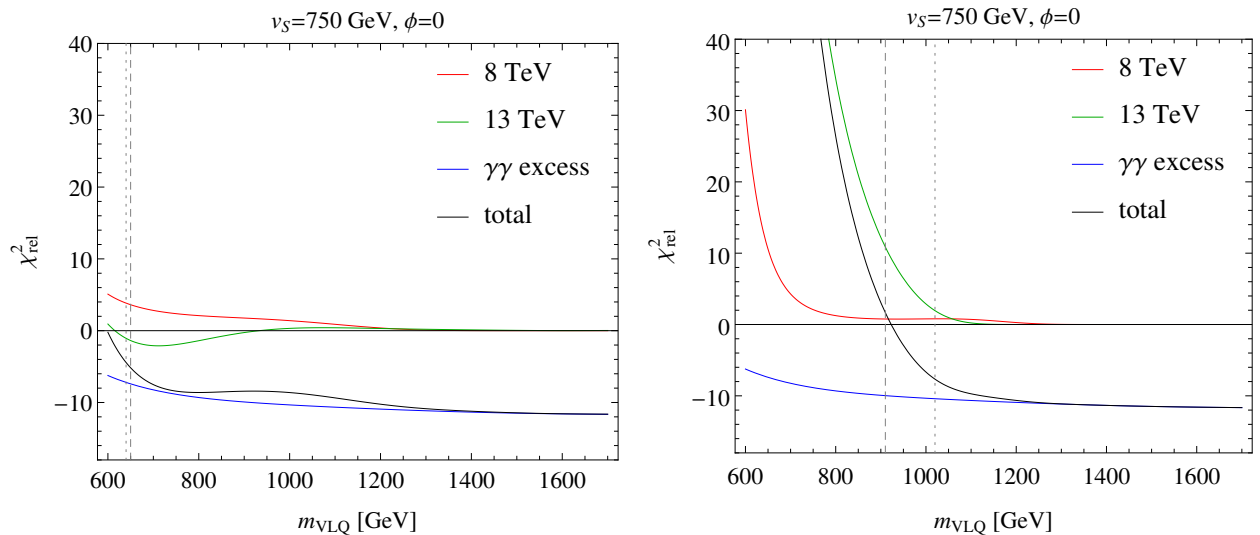


Figure 5. Fit of vector-like quark doublet (X, T) coupling to the first (left) and third (right) generation of SM quarks. The individual contributions to the likelihood from comparison to the 8 TeV and 13 TeV analyses for pair production of VLQs with **CheckMATE** and the fit to the diphoton excess are also shown. The dashed (dotted) line marks the limit on the VLQ mass obtained using the CLs method (single sided 95% limit).

[¶] We do not show the LHC results for the other models here since the (T, B) model is unable to explain the diphoton excess and the (B, Y) model requires $m_{\text{VLQ}} < 600$ GeV which can be clearly seen to be ruled out by Fig. 5. (Note that the possible presence of b -quarks in the final state will actually tighten the bounds compared to those shown.)

In a model where the VLQs couple only to the first generation of SM quarks, the 8 TeV analyses (mostly the ‘vanilla’ ATLAS jets and E_T^{miss} SUSY search [54]) are found to provide the strongest constraints. It is not surprising that the SUSY search produces the most stringent limit in these cases since the dedicated VLQ search is designed to only look for top-like partners that decay into the third generation and consequently produce a number of b-jets in the final state. In contrast the SUSY search does not require b-jets.

One may wonder why the 8 TeV search gives a stronger limit than the same search does at 13 TeV and this is mainly due to the fact that the 13 TeV search has significantly increased both the individual jet p_T thresholds and the required minimum value of the variable named m_{eff} (sum of jet p_T and E_T^{miss}). For example, the strongest 8 TeV limit comes from the 5 jet signal region which requires a hardest jet, $p_T > 130$ GeV and $m_{\text{eff}} > 1200$ GeV. In contrast, at 13 TeV these thresholds have been increased to $p_T > 200$ GeV and $m_{\text{eff}} > 1600$ GeV which substantially reduces the acceptance for our VLQ states.

Using just a single signal region we find a limit using the CLs method of $m_{\text{VLQ}} \gtrsim 650$ GeV on the VLQ states that couple to light quarks. One may find such a result surprising since one might naively think that VLQ production does not produce a significant E_T^{miss} signature. However we find that the neutrinos from $Z \rightarrow \nu\nu$ and $W \rightarrow \ell\nu$, combined with the large production cross-section, do in fact make the supersymmetric searches sensitive to VLQ production. In addition it is clear that an optimized search for such states would produce significantly enhanced constraints. In particular we believe that exploiting possible resonant structures in this regard may be very profitable and these will be explored in a future study**.

Instead of only using a single signal region, we can alternatively combine all of the orthogonal signal regions in the study and define the VLQ state as being excluded when the fit is $1.64\text{-}\sigma$ worse than the Standard Model (single sided 95% limit). The combination actually leads to a slightly weaker bound of $m_{\text{VLQ}} \gtrsim 640$ GeV; the reason for this is that the ATLAS on-shell Z + MET excess prefers the production of VLQs near this mass range. However, we should emphasize that the excess is not statistically significant and we will further discuss this result later in this Section.

Nevertheless, when fitting the model to the complete VLQ/SUSY search data set, and including also the diphoton signal, we find a large improvement in the fit quality for the entire range of VLQ masses investigated, Fig. 5(right). The reason is the strength of the diphoton signal and the $\sim 3.9\sigma$ excess that is seen over the Standard Model prediction. Due to the fact that when $\phi = 0$ and $v_S = 750$ GeV, the (X, T) model predicts a too high diphoton cross-section, we see that the best fit continues to improve as we increase the VLQ mass.

If we now examine the limits in the case where the (X, T) model instead couples to the third generation we see that the bounds are significantly tighter, Fig. 5(left). The reason is that both the X and T states will decay via on-shell top quarks (and Higgs Bosons) and these (or the produced b-quarks) are used by many searches as a way to reduce SM background.

More surprising is the result that the largest sensitivity and thus the tightest bound on the VLQ states *does not* come from the dedicated VLQ search [12] which focuses on $T\bar{T}$ production, but instead from the ATLAS 13 TeV search for gluinos [55] with at least $3b$ -jets and E_T^{miss} , Fig. 6. For example, the limit at 95% CLs from this supersymmetric search is $m_{\text{VLQ}} \gtrsim 910$ GeV whereas the limit from the dedicated VLQ search is only $m_{\text{VLQ}} \gtrsim 825$ GeV, so that the supersymmetric search channel provides a much more stringent constraint! The difference in these two searches is that the VLQ search is inclusive and only targets final states with high jet multiplicity (and 1-lepton). In contrast, the supersymmetric search requires significant E_T^{miss} as well as m_{eff} which successfully suppresses the SM background.

** As stated in the introduction, in the finishing stages of this study ATLAS released an analysis sensitive to VLQs that included missing energy as a discriminator[15].

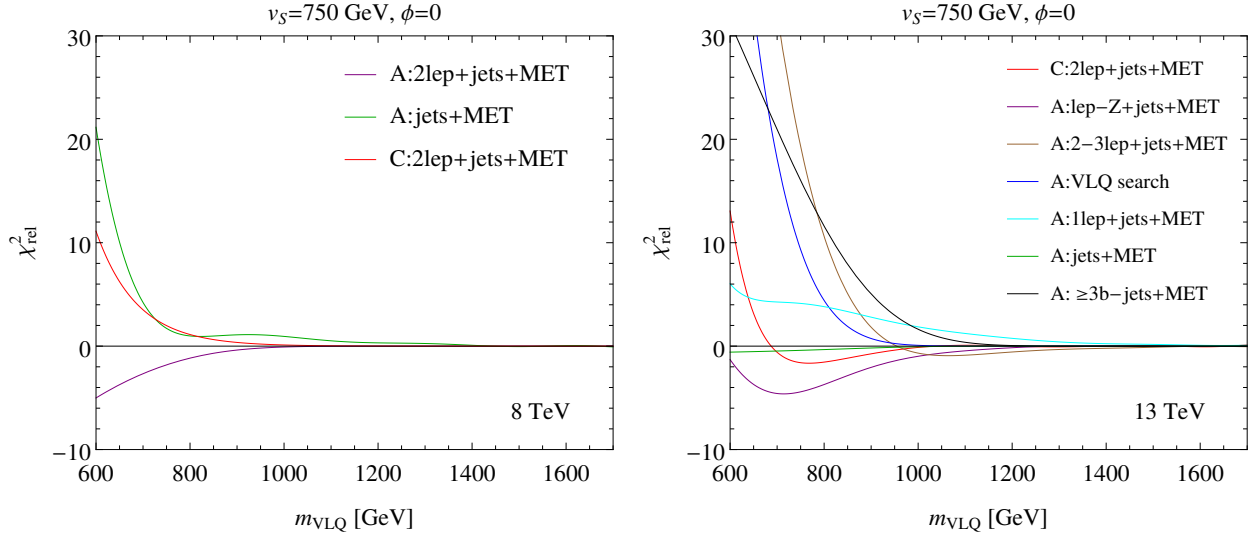


Figure 6. Individual contributions (A=ATLAS and C=CMS) from different LHC searches at 8 TeV (left) and 13 TeV (right) to the relative χ^2 for the (X, T) doublet model coupling to the third generation of SM quarks.

The signal regions of the supersymmetric search which set the tightest limit on this model are ‘Gtt-1L-A’ and ‘Gtt-1L-B’. They require 1 lepton in the final state together with $E_T^{\text{miss}} > 200/300$ GeV and $m_{\text{eff}} > 1100/900$ GeV respectively.

The above results show that missing energy from $Z \rightarrow \nu\nu$ and $W \rightarrow \ell\nu$ that are produced in the VLQ decays should be much further investigated so as to improve sensitivity to these models. Conventionally, missing energy has not been considered as important in searches for VLQs but the fact that a supersymmetric search that has been optimized for gluinos outperforms the dedicated VLQ search as found here demonstrates that this is probably misguided.

From the combination of all orthogonal signal regions we obtain a single sided 95% limit of $m_{\text{VLQ}} \gtrsim 1020$ GeV. This limit is stronger than the one obtained with the CLs method, for two main reasons. Firstly we have combined all analyses together and this leads to a stronger bound than only considering the best expected limit from a single signal region. Secondly, and more importantly, the ATLAS 13 TeV search for gluinos with at least 3b-jets that is most constraining has found several under-fluctuations in the relevant signal regions. The commonly used CLs method ‘punishes’ the exclusion when such under-fluctuations occur but this is not the case in the combined likelihood method that we have used here and thus a much stronger limit is obtained.

If we further examine Fig. 6, we can see that at both 8 and 13 TeV the excess that is present in the ATLAS on-shell Z+MET gluino search by the negative χ^2 contribution to the fit. Taking into account the other searches we have investigated it is already clear that any VLQ explanation for this excess does not improve the overall fit of the model.

Nevertheless, in Fig. 7 we now only consider the same ATLAS and CMS signal regions at 13 TeV and the most similar regions at 8 TeV. We see that at 8 TeV, the constraint coming from the non-observation of the excess in CMS almost exactly cancels that from the positive ATLAS result. At 13 TeV, the constraint from CMS is not quite as strong but we still see that the peak significance is reduced to just 1.5- σ and we therefore do not investigate this excess further.

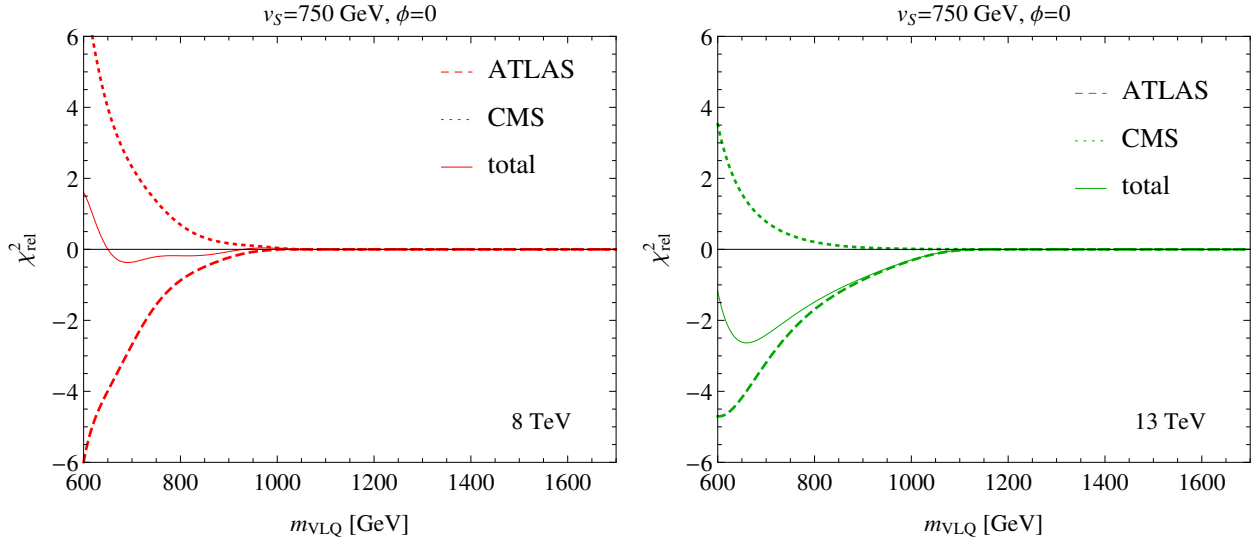


Figure 7. Contributions to the likelihood obtained from comparison of the predictions to the signal region results sensitive to the ATLAS on-Z excess at 8 TeV (left) and 13 TeV (right) for the (X, T) model.

C. Global Fit

In order to understand the model parameters that best fit all of the available data we now combine our fit of the diphoton signal with the likelihood given by the LHC searches for VLQ production. Since only the (X, T) model was able to fit the diphoton excess whilst simultaneously not being excluded by the direct VLQ searches, we now ignore the other models. In addition, since the decays of the VLQ states depend on the generation of the Standard Model quarks we now separately discuss the cases where they primarily couple to the first and third generation.

In the upper row of Fig. 8 we display the case where the VLQs couple to the first generation. Comparing with Fig. 4 (lower) we see that the effect of adding the direct production LHC searches is to disfavor models with smaller VLQ masses. More precisely, models with $m_{\text{VLQ}} \lesssim 630$ GeV are now ruled out at the $3\text{-}\sigma$ level. The best fit region is found for large VLQ masses and the main $1\text{-}\sigma$ region is found for $m_{\text{VLQ}} \gtrsim 1100$ GeV. Large VLQ masses are preferred for two reasons with the first being that the direct searches for these states disfavor lower masses. Secondly, in the (X, T) model with no scalar mixing and $v_S = 875$ GeV, the model actually predicts a too high diphoton rate, and increasing the VLQ mass somewhat reduces the production cross-section.

As explained before, an alternative way to reduce the diphoton rate is to increase the mixing angle with the SM Higgs to be in the (absolute) range 0.01–0.02. The introduction of the mixing allows additional decay modes to enter while boosting others and thus produces a better fit. An increase in v_S also reduces the diphoton rate but is compensated here as the VLQ scalar coupling is smaller for fixed m_{VLQ} . A final feature to note in the best fit contours is that a lighter VLQ region, $700 \lesssim m_{\text{VLQ}} \lesssim 850$ GeV, is compatible with the best fit at $1\text{-}\sigma$. The reason for the existence of this region is that the $1.5\text{-}\sigma$ on-shell $Z+\text{MET}$ ATLAS excess marginally improves the agreement with data here.

Moving on to the case where the (X, T) states couple to the third generation, the effect of the LHC searches for VLQ states is far more severe. We now see in Fig. 8 (lower), that models with $m_{\text{VLQ}} \lesssim 1050$ GeV are excluded at the $3\text{-}\sigma$ level. Again we also note that either a non-zero scalar mixing angle or a $v_S \gtrsim 900$ GeV are required to fit the diphoton excess in the region of VLQ masses studied in this analysis.

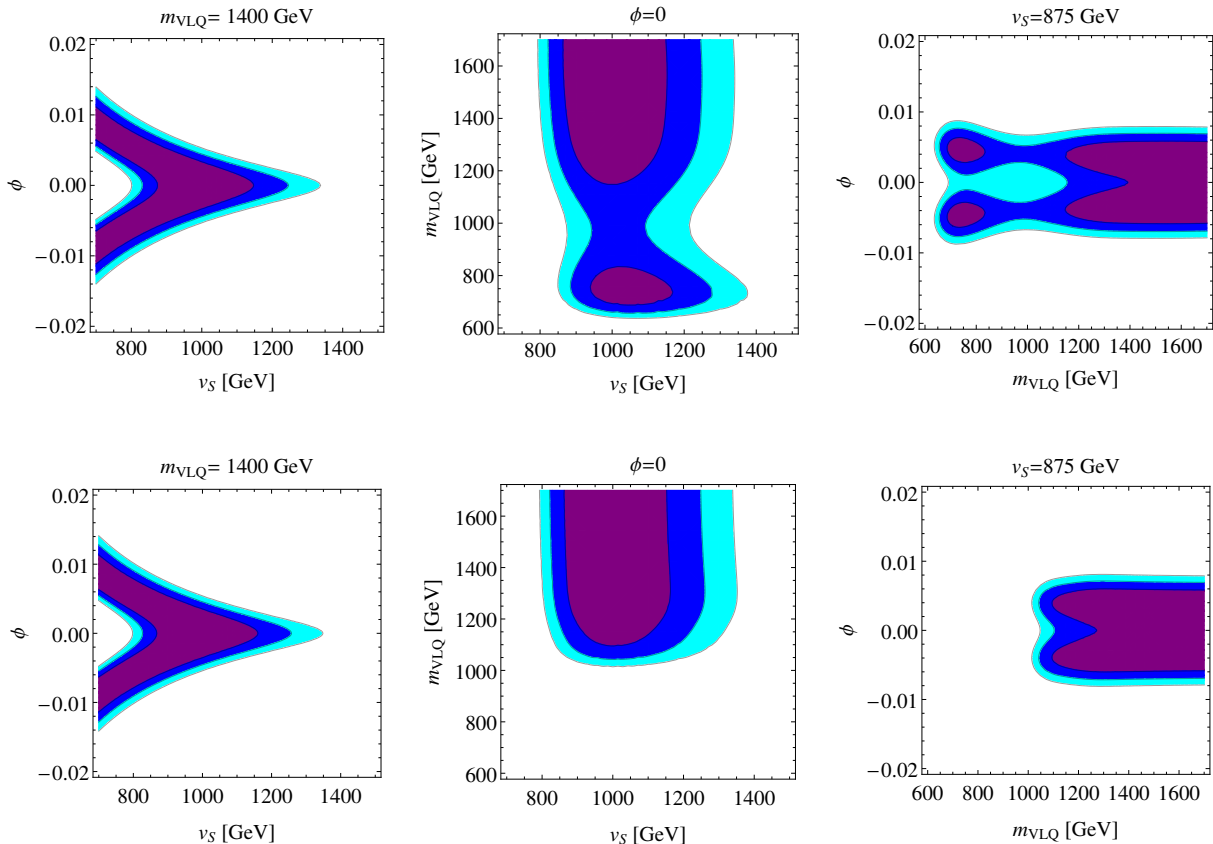


Figure 8. Contours of the likelihood for the (X, T) model for the diphoton contribution taking into account the constraints from VLQ pair production for VLQs coupling to the first (upper) or third (lower) generation of SM fermions. The contours are shown for the 1σ (purple), 2σ (dark blue) and 3σ (light blue) regions.

IV. SUMMARY

In this paper we have examined a model containing an additional scalar singlet and a new vector-like quark doublet in order to explore the complementarity of a variety of LHC searches for new states. Both the production and decay of the scalar singlet is mediated by the VLQ loop. This scenario is employed as an example simplified model and could also explain the earlier reported diphoton excess observed by the ATLAS and CMS collaborations. Furthermore, we employed a number of direct LHC searches for supersymmetric partners and the VLQs themselves. Using **CheckMATE** we showed how this scenario could be tested and its parameters probed using data from the 8 and 13 TeV runs of the LHC.

As a very concrete example, we analyzed the models corresponding to the three possible charge assignments for the VLQ doublet extension where the VLQ states can also couple to the SM Higgs and the VLQs then decay via mixing with their SM partners with the same quantum numbers. Two of these models, with either a (B, Y) or (T, B) doublet, predict a diphoton production rate which is too small to explain the apparent excess. However, with the (X, T) doublet scenario, we demonstrated that we were able to reproduce correctly the size of the apparent excess and impose bounds on the masses and couplings of the VLQ, as well as the vacuum expectation value of the singlet scalar and its mixing with SM-like Higgs boson.

Applying the various VLQ and supersymmetric searches, we found that additional constraints

are then placed on the model to significantly limit the possible parameter space. In the case where the VLQ was assumed to mix predominantly to the first generation of SM fermions we found that the 8 TeV supersymmetric search for jets plus missing energy provided the strongest constraints and set a lower limit of $m_{\text{VLQ}} \gtrsim 650$ GeV. The fact that the 8 TeV limit was found to be stronger than that derived from the combination of the 13 TeV searches we investigated motivates a dedicated 13 TeV effort to constrain such a model.

When the VLQ states mixed predominantly to the third generation SM fermions, we found that the resulting limits were much stronger requiring that $m_{\text{VLQ}} \gtrsim 910$ GeV. More importantly, however, we found that the 3- b jet supersymmetric search with missing energy is significantly more sensitive to the production of these new VLQ states than was the dedicated VLQ search itself! This result motivates a possible re-appraisal of the general VLQ search strategy to examine whether including missing energy as a discriminator can help increase sensitivity to these types of models.

In conclusion, we have demonstrated the importance of complementarity of LHC searches for new physics and urge our experimental colleagues to employ this principle in developing their search analyses.

Acknowledgments

We would like to thank Tim Keller and Jan Schütte-Engel for the implementation of LHC searches into **CheckMATE**. JSK thanks Thomas Flacke for discussions. KR is supported by the National Science Centre (Poland) under Grant 2015/19/D/ST2/03136 and the Collaborative Research Center SFB676 of the DFG, “Particles, Strings, and the Early Universe.” The work of JSK has been partially supported by the MINECO, Spain, under contract FPA2013-44773-P; Consolider-Ingenio CPAN CSD2007-00042 and the Spanish MINECO Centro de excelencia Severo Ochoa Program under grant SEV-2012-0249. MK and JT have been supported in part by the DFG Research Unit 2239 “New Physics at the Large Hadron Collider.” The work of JLH and TGR was supported by the U.S. Department of Energy Office of Science, Contract DE-AC02-76SF00515.

Appendix A: Additional decay modes of h_2

Here we provide the components of the tree level decays of h_2 which are induced by a finite mixing ($\phi \neq 0$) with the SM Higgs:

$$\Gamma(h_2 \rightarrow h_1 h_1) = \frac{s_\phi^2 c_\phi^2 M_{h_2}^3}{32\pi v_H^2} \left(c_\phi + s_\phi \frac{v_H}{v_S} \right)^2 (1 + 2u_{h_1})^2 \sqrt{1 - 4u_{h_1}}, \quad u_x = \frac{M_x^2}{M_{h_2}^2}, \quad (\text{A1})$$

$$\Gamma(h_2 \rightarrow t\bar{t}) = \frac{3s_\phi^2 M_{h_2} m_t^2}{8\pi v_H^2} (1 - 4u_t)^2 \sqrt{1 - 4u_t}, \quad (\text{A2})$$

$$\Gamma(h_2 \rightarrow ZZ)|_{\text{tree}} = \frac{s_\phi^2 G_F^2 v_H^2 M_{h_2}^3}{16\pi} (1 - 4u_Z + 12u_Z^2) \sqrt{1 - 4u_Z}, \quad (\text{A3})$$

$$\Gamma(h_2 \rightarrow WW)|_{\text{tree}} = \frac{s_\phi^2 G_F^2 v_H^2 M_{h_2}^3}{8\pi} (1 - 4u_W + 12u_W^2) \sqrt{1 - 4u_W}. \quad (\text{A4})$$

[1] S. Arrenberg *et al.*, “Working Group Report: Dark Matter Complementarity,” in *Community Summer Study 2013: Snowmass on the Mississippi (CSS2013) Minneapolis, MN, USA, July*

- 29-August 6, 2013. 2013. [arXiv:1310.8621](https://arxiv.org/abs/1310.8621) [hep-ph].
<https://inspirehep.net/record/1262784/files/arXiv:1310.8621.pdf>.
- [2] M.-L. Xiao and J.-H. Yu, “Stabilizing electroweak vacuum in a vectorlike fermion model,” *Phys. Rev. D* **90** (2014) no. 1, 014007, [arXiv:1404.0681](https://arxiv.org/abs/1404.0681) [hep-ph]. [Addendum: *Phys. Rev. D* **90**, no. 1, 019901 (2014)].
 - [3] M. J. Dolan, J. L. Hewett, M. Krämer, and T. G. Rizzo, “Simplified Models for Higgs Physics: Singlet Scalar and Vector-like Quark Phenomenology,” *JHEP* **07** (2016) 039, [arXiv:1601.07208](https://arxiv.org/abs/1601.07208) [hep-ph].
 - [4] ATLAS Collaboration, M. Aaboud *et al.*, “Search for resonances in diphoton events at $\sqrt{s}=13$ TeV with the ATLAS detector,” [arXiv:1606.03833](https://arxiv.org/abs/1606.03833) [hep-ex].
 - [5] CMS Collaboration, V. Khachatryan *et al.*, “Search for resonant production of high-mass photon pairs in proton-proton collisions at $\sqrt{s} = 8$ and 13 TeV,” [arXiv:1606.04093](https://arxiv.org/abs/1606.04093) [hep-ex].
 - [6] R. Benbrik, C.-H. Chen, and T. Nomura, “Higgs singlet boson as a diphoton resonance in a vectorlike quark model,” *Phys. Rev. D* **93** (2016) no. 5, 055034, [arXiv:1512.06028](https://arxiv.org/abs/1512.06028) [hep-ph].
 - [7] W. Chao, R. Huo, and J.-H. Yu, “The Minimal Scalar-Stealth Top Interpretation of the Diphoton Excess,” [arXiv:1512.05738](https://arxiv.org/abs/1512.05738) [hep-ph].
 - [8] A. Angelescu, A. Djouadi, and G. Moreau, “Scenarii for interpretations of the LHC diphoton excess: two Higgs doublets and vector-like quarks and leptons,” *Phys. Lett. B* **756** (2016) 126–132, [arXiv:1512.04921](https://arxiv.org/abs/1512.04921) [hep-ph].
 - [9] P. S. B. Dev, R. N. Mohapatra, and Y. Zhang, “Quark Seesaw, Vectorlike Fermions and Diphoton Excess,” *JHEP* **02** (2016) 186, [arXiv:1512.08507](https://arxiv.org/abs/1512.08507) [hep-ph].
 - [10] J. A. Aguilar-Saavedra, R. Benbrik, S. Heinemeyer, and M. Prez-Victoria, “Handbook of vectorlike quarks: Mixing and single production,” *Phys. Rev. D* **88** (2013) no. 9, 094010, [arXiv:1306.0572](https://arxiv.org/abs/1306.0572) [hep-ph].
 - [11] M. Buchkremer, G. Cacciapaglia, A. Deandrea, and L. Panizzi, “Model Independent Framework for Searches of Top Partners,” *Nucl. Phys. B* **876** (2013) 376–417, [arXiv:1305.4172](https://arxiv.org/abs/1305.4172) [hep-ph].
 - [12] ATLAS Collaboration, G. Aad *et al.*, “Search for production of vector-like top quark pairs and of four top quarks in the lepton-plus-jets final state in pp collisions at $\sqrt{s} = 13$ TeV with the ATLAS detector,”.
 - [13] D. Barducci, A. Belyaev, M. Buchkremer, J. Marrouche, S. Moretti, and L. Panizzi, “XQCAT: eXtra Quark Combined Analysis Tool,” *Comput. Phys. Commun.* **197** (2015) 263–275, [arXiv:1409.3116](https://arxiv.org/abs/1409.3116) [hep-ph].
 - [14] S. Kraml, U. Laa, L. Panizzi, and H. Prager, “Scalar versus fermionic top partner interpretations of $t\bar{t} + E_T^{\text{miss}}$ searches at the LHC,” [arXiv:1607.02050](https://arxiv.org/abs/1607.02050) [hep-ph].
 - [15] ATLAS Collaboration, T. A. collaboration, “Search for new physics using events with b -jets and a pair of same charge leptons in 3.2 fb^{-1} of pp collisions at $\sqrt{s} = 13$ TeV with the ATLAS detector,”.
 - [16] ATLAS Collaboration, G. Aad *et al.*, “Search for supersymmetry in events containing a same-flavour opposite-sign dilepton pair, jets, and large missing transverse momentum in $\sqrt{s} = 8$ TeV pp collisions with the ATLAS detector,” *Eur. Phys. J. C* **75** (2015) no. 7, 318, [arXiv:1503.03290](https://arxiv.org/abs/1503.03290) [hep-ex]. [Erratum: *Eur. Phys. J. C* **75**, no. 10, 463 (2015)].
 - [17] ATLAS Collaboration, G. Aad *et al.*, “A search for Supersymmetry in events containing a leptonically decaying Z boson, jets and missing transverse momentum in $\sqrt{s} = 13$ TeV pp collisions with the ATLAS detector,”.
 - [18] M. Endo and Y. Takaesu, “ATLAS on-Z Excess Through Vector-Like Quarks,” *Phys. Lett. B* **758** (2016) 355–358, [arXiv:1602.05075](https://arxiv.org/abs/1602.05075) [hep-ph].
 - [19] CMS Collaboration, V. Khachatryan *et al.*, “Search for Physics Beyond the Standard Model in Events with Two Leptons, Jets, and Missing Transverse Momentum in pp Collisions at $\sqrt{s} = 8$ TeV,” *JHEP* **04** (2015) 124, [arXiv:1502.06031](https://arxiv.org/abs/1502.06031) [hep-ex].
 - [20] CMS Collaboration, V. Khachatryan *et al.*, “Search for new physics in final states with two opposite-sign, same-flavor leptons, jets, and missing transverse momentum in pp collisions at $\sqrt{s} = 13$ TeV,” [arXiv:1607.00915](https://arxiv.org/abs/1607.00915) [hep-ex].
 - [21] N. V. Krasnikov, “Invisible scalars visible in Higgs decay,” *Phys. Lett. B* **291** (1992) 89–91.
 - [22] D. O’Connell, M. J. Ramsey-Musolf, and M. B. Wise, “Minimal Extension of the Standard Model Scalar Sector,” *Phys. Rev. D* **75** (2007) 037701, [arXiv:hep-ph/0611014](https://arxiv.org/abs/hep-ph/0611014) [hep-ph].
 - [23] V. Barger, P. Langacker, M. McCaskey, M. J. Ramsey-Musolf, and G. Shaughnessy, “LHC Phenomenology of an Extended Standard Model with a Real Scalar Singlet,” *Phys. Rev. D* **77** (2008)

- 035005, [arXiv:0706.4311 \[hep-ph\]](#).
- [24] V. Barger, P. Langacker, M. McCaskey, M. Ramsey-Musolf, and G. Shaughnessy, “Complex Singlet Extension of the Standard Model,” *Phys. Rev.* **D79** (2009) 015018, [arXiv:0811.0393 \[hep-ph\]](#).
- [25] B. Batell, S. Jung, and H. M. Lee, “Singlet Assisted Vacuum Stability and the Higgs to Diphoton Rate,” *JHEP* **01** (2013) 135, [arXiv:1211.2449 \[hep-ph\]](#).
- [26] C.-Y. Chen, S. Dawson, and Y. Zhang, “Higgs CP Violation from Vectorlike Quarks,” *Phys. Rev.* **D92** (2015) no. 7, 075026, [arXiv:1507.07020 \[hep-ph\]](#).
- [27] A. K. Alok, S. Banerjee, D. Kumar, S. U. Sankar, and D. London, “New-physics signals of a model with a vector-singlet up-type quark,” *Phys. Rev.* **D92** (2015) 013002, [arXiv:1504.00517 \[hep-ph\]](#).
- [28] **SLD Electroweak Group, DELPHI, ALEPH, SLD, SLD Heavy Flavour Group, OPAL, LEP Electroweak Working Group, L3** Collaboration, S. Schael *et al.*, “Precision electroweak measurements on the Z resonance,” *Phys. Rept.* **427** (2006) 257–454, [arXiv:hep-ex/0509008 \[hep-ex\]](#).
- [29] A. Deandrea, “Atomic parity violation in cesium and implications for new physics,” *Phys. Lett.* **B409** (1997) 277–282, [arXiv:hep-ph/9705435 \[hep-ph\]](#).
- [30] M. E. Peskin and T. Takeuchi, “A New constraint on a strongly interacting Higgs sector,” *Phys. Rev. Lett.* **65** (1990) 964–967.
- [31] P. Bamert, C. P. Burgess, J. M. Cline, D. London, and E. Nardi, “ $R(b)$ and new physics: A Comprehensive analysis,” *Phys. Rev.* **D54** (1996) 4275–4300, [arXiv:hep-ph/9602438 \[hep-ph\]](#).
- [32] M. Cirelli and A. Strumia, “Minimal Dark Matter: Model and results,” *New J. Phys.* **11** (2009) 105005, [arXiv:0903.3381 \[hep-ph\]](#).
- [33] S. Knapen, T. Melia, M. Papucci, and K. Zurek, “Rays of light from the LHC,” *Phys. Rev.* **D93** (2016) no. 7, 075020, [arXiv:1512.04928 \[hep-ph\]](#).
- [34] X. Liu and H. Zhang, “RG-improved Prediction for 750 GeV Resonance Production at the LHC,” [arXiv:1603.07190 \[hep-ph\]](#).
- [35] A. Djouadi, M. Spira, and P. M. Zerwas, “Production of Higgs bosons in proton colliders: QCD corrections,” *Phys. Lett.* **B264** (1991) 440–446.
- [36] A. Alloul, N. D. Christensen, C. Degrande, C. Duhr, and B. Fuks, “FeynRules 2.0 - A complete toolbox for tree-level phenomenology,” *Comput. Phys. Commun.* **185** (2014) 2250–2300, [arXiv:1310.1921 \[hep-ph\]](#).
- [37] N. D. Christensen and C. Duhr, “FeynRules - Feynman rules made easy,” *Comput. Phys. Commun.* **180** (2009) 1614–1641, [arXiv:0806.4194 \[hep-ph\]](#).
- [38] M. Drees, H. Dreiner, D. Schmeier, J. Tattersall, and J. S. Kim, “CheckMATE: Confronting your Favourite New Physics Model with LHC Data,” *Comput. Phys. Commun.* **187** (2015) 227–265, [arXiv:1312.2591 \[hep-ph\]](#).
- [39] J. S. Kim, D. Schmeier, J. Tattersall, and K. Rolbiecki, “A framework to create customised LHC analyses within CheckMATE,” *Comput. Phys. Commun.* **196** (2015) 535–562, [arXiv:1503.01123 \[hep-ph\]](#).
- [40] **DELPHES 3** Collaboration, J. de Favereau, C. Delaere, P. Demin, A. Giammanco, V. Lematre, A. Mertens, and M. Selvaggi, “DELPHES 3, A modular framework for fast simulation of a generic collider experiment,” *JHEP* **02** (2014) 057, [arXiv:1307.6346 \[hep-ex\]](#).
- [41] M. Cacciari, G. P. Salam, and G. Soyez, “FastJet User Manual,” *Eur. Phys. J.* **C72** (2012) 1896, [arXiv:1111.6097 \[hep-ph\]](#).
- [42] M. Cacciari and G. P. Salam, “Dispelling the N^3 myth for the k_t jet-finder,” *Phys. Lett.* **B641** (2006) 57–61, [arXiv:hep-ph/0512210 \[hep-ph\]](#).
- [43] M. Cacciari, G. P. Salam, and G. Soyez, “The Anti- $k(t)$ jet clustering algorithm,” *JHEP* **04** (2008) 063, [arXiv:0802.1189 \[hep-ph\]](#).
- [44] J. Cao, L. Shang, J. M. Yang, and Y. Zhang, “Explanation of the ATLAS Z-Peaked Excess in the NMSSM,” *JHEP* **06** (2015) 152, [arXiv:1504.07869 \[hep-ph\]](#).
- [45] M. R. Buckley, “Wide or narrow? The phenomenology of 750 GeV diphotons,” *Eur. Phys. J.* **C76** (2016) no. 6, 345, [arXiv:1601.04751 \[hep-ph\]](#).
- [46] J. Alwall, R. Frederix, S. Frixione, V. Hirschi, F. Maltoni, O. Mattelaer, H. S. Shao, T. Stelzer, P. Torrielli, and M. Zaro, “The automated computation of tree-level and next-to-leading order differential cross sections, and their matching to parton shower simulations,” *JHEP* **07** (2014) 079, [arXiv:1405.0301 \[hep-ph\]](#).

- [47] **ATLAS** Collaboration, G. Aad *et al.*, “Search for a high-mass Higgs boson decaying to a W boson pair in pp collisions at $\sqrt{s} = 8$ TeV with the ATLAS detector,” *JHEP* **01** (2016) 032, [arXiv:1509.00389](#) [[hep-ex](#)].
- [48] **ATLAS** Collaboration, G. Aad *et al.*, “Search for an additional, heavy Higgs boson in the $H \rightarrow ZZ$ decay channel at $\sqrt{s} = 8$ TeV in pp collision data with the ATLAS detector,” *Eur. Phys. J.* **C76** (2016) no. 1, 45, [arXiv:1507.05930](#) [[hep-ex](#)].
- [49] **ATLAS** Collaboration, G. Aad *et al.*, “Search for new phenomena in the dijet mass distribution using $p - p$ collision data at $\sqrt{s} = 8$ TeV with the ATLAS detector,” *Phys. Rev.* **D91** (2015) no. 5, 052007, [arXiv:1407.1376](#) [[hep-ex](#)].
- [50] **ATLAS** Collaboration, G. Aad *et al.*, “Search for new resonances in $W\gamma$ and $Z\gamma$ final states in pp collisions at $\sqrt{s} = 8$ TeV with the ATLAS detector,” *Phys. Lett.* **B738** (2014) 428–447, [arXiv:1407.8150](#) [[hep-ex](#)].
- [51] **ATLAS** Collaboration, G. Aad *et al.*, “Searches for Higgs boson pair production in the $hh \rightarrow bb\tau\tau, \gamma\gamma WW^*, \gamma\gamma bb, bbbb$ channels with the ATLAS detector,” *Phys. Rev.* **D92** (2015) 092004, [arXiv:1509.04670](#) [[hep-ex](#)].
- [52] T. Sjostrand, S. Mrenna, and P. Z. Skands, “PYTHIA 6.4 Physics and Manual,” *JHEP* **05** (2006) 026, [arXiv:hep-ph/0603175](#) [[hep-ph](#)].
- [53] M. Czakon and A. Mitov, “Top++: A Program for the Calculation of the Top-Pair Cross-Section at Hadron Colliders,” *Comput. Phys. Commun.* **185** (2014) 2930, [arXiv:1112.5675](#) [[hep-ph](#)].
- [54] **ATLAS** Collaboration, G. Aad *et al.*, “Search for squarks and gluinos with the ATLAS detector in final states with jets and missing transverse momentum using $\sqrt{s} = 8$ TeV proton–proton collision data,” *JHEP* **09** (2014) 176, [arXiv:1405.7875](#) [[hep-ex](#)].
- [55] **ATLAS** Collaboration, G. Aad *et al.*, “Search for pair-production of gluinos decaying via stop and sbottom in events with b -jets and large missing transverse momentum in $\sqrt{s} = 13$ TeV pp collisions with the ATLAS detector,”.
- [56] **ATLAS** Collaboration, G. Aad *et al.*, “Search for gluinos in events with an isolated lepton, jets and missing transverse momentum at $\sqrt{s} = 13$ TeV with the ATLAS detector,” [arXiv:1605.04285](#) [[hep-ex](#)].
- [57] **ATLAS** Collaboration, G. Aad *et al.*, “Search for squarks and gluinos in final states with jets and missing transverse momentum at $\sqrt{s} = 13$ TeV with the ATLAS detector,”.
- [58] **ATLAS** Collaboration, G. Aad *et al.*, “Search for supersymmetry at $\sqrt{s} = 13$ TeV in final states with jets and two same-sign leptons or three leptons with the ATLAS detector,” *Eur. Phys. J.* **C76** (2016) no. 5, 259, [arXiv:1602.09058](#) [[hep-ex](#)].